Soil-dependent β and γ shape parameters of the Haverkamp infiltration model for 3D infiltration flow

D. Yilmaz, L. Lassabatere, D. Moret-Fernandez, M. Rahmati, R. Angulo-Jaramillo, B. Latorre

Soil-dependent β and γ shape parameters of the Haverkamp infiltration model for 3D infiltration flow

D. Yilmaz[a], L. Lassabatere[b], D. Moret-Fernandez[c], M. Rahmati[d,e], R. Angulo-Jaramillo[b], and B. Latorre[c]

[a] Civil Engineering Department, Engineering Faculty, Munzur University, Tunceli, Turkey

[b] Université de Lyon; UMR5023 Ecologie des Hydrosystèmes Naturels et Anthropisés, CNRS, ENTPE, Université Lyon 1, Vaulx-en-Velin, France.

[c] Departamento de Suelo y Agua, Estación Experimental de Aula Dei, Consejo Superior de Investigaciones Científicas (CSIC), PO Box 13034, 50080 Zaragoza, Spain

[d] Department of Soil Science and Engineering, Faculty of Agriculture, University of Maragheh, Maragheh, Iran

[e] Forschungszentrum Jülich GmbH, Institute of Bio- and Geosciences: Agrosphere (IBG-3), Jülich, Germany

Highlights

- Our approach allowed robust estimation of (β, γ) couplet
- Six synthetic soils and different initial scenarios of soil water content were considered
- The (β, γ) couplet was proved dependent on the type of soil and initial condition
- New prefixed (β, γ) values are more reliable for S and K_s accurate estimations

Abstract:

Estimating of soil sorptivity (S) and saturated hydraulic conductivity (K_s) parameters by field infiltration tests are widespread due to the ease of the experimental protocol and data treatment. The analytical equation proposed by Haverkamp et al. (1994) allows the modeling of the cumulative infiltration process, from which the hydraulic parameters can be estimated. This model depends on both initial and final values of the soil hydraulic conductivity, initial soil sorptivity, the volumetric water content increase ($\Delta\theta$), and two infiltration constants, the so-called β and γ parameters. However, to reduce the number of unknown variables when inverting experimental data, constant parameters such

as β and γ are usually prefixed to 0.6 and 0.75, respectively. In this study, the values of these constants are investigated using numerical infiltration curves for different soil types and initial soil water contents for the van Genuchten-Mualem (vGM) soil hydraulic model. Our approach considers the long-time expansions of the Haverkamp model, the exact soil properties such as S, K_s, and initial soil moisture to derive the value of the β and γ parameters for each specific case. We then generated numerically cumulative infiltration curves using Hydrus 3-D software and fitted the long-time expansions to derive the value of the β and γ parameters. The results show that these parameters are influenced by the initial soil water content and the soil type. However, for initially dry soil conditions, some prefixed values can be proposed instead of the currently used values. If an accurate estimate of S and K_s is the case, then for coarse-textured soils such as sand and loamy sand, we propose the use of 0.9 for both constants. For the remaining soils, the value of 0.75 can be retained for γ. For β constant, 0.75 and 1.5 values can be considered for, intermediate permeable soils (sandy loam and loam) and low permeable soils (silty loam and silt), respectively. We clarify that the results are based on using the vGM model to describe the hydraulic functions of the soil and that the results may differ, and the assumptions may change for other models.

Keywords: Beerkan infiltration, soil sorptivity, saturated hydraulic conductivity, Haverkamp model, steady-state, Hydrus 3D synthetic soils.

1- Introduction

The quasi-exact implicit (QEI) three-dimensional (3D) analytical formulation for a disc infiltrometer infiltration with null or negative surface pressure (Haverkamp et al., 1994) is derived from the one-dimensional (1D) analytic approximation (AAP) proposed by Parlange et al. (1982), by including a new term representing the lateral flow (Smettem et al., 1994). This equation is expressed as a function of soil sorptivity, S, and hydraulic conductivity, K, volumetric water content increase, $\Delta\theta$, and integration β and scale γ parameters.

The β parameter, which was initially introduced by Parlange et al. (1982) to derive the general form of the 1D QEI formulation, was next redefined by Haverkamp et al. (1990). According to Haverkamp et al. (1994), β is a function of the soil hydraulic conductivity, the soil diffusivity, and the initial and final volumetric water content. As for the constant β, several studies (Ross et al., 1996; Haverkamp et al., 1999) found it to be in the range of [0, 1], where 0 corresponds to soils with Green-Ampt (GA) behavior, and one corresponds to very diffusive soils. This gave a physical interpretation to the integration parameter β depending on the soil type. However, the constant β value of 0.6 initially retained by Haverkamp et al. (1994), which was specific to their studied experimental sandy loam soil, became a default setting in almost all studies (Angulo-Jaramillo et al., 2016). This "0.6" value was calculated using soil textural information and the 1D analytical formulation (Fuentes et al., 1992). Some works have numerically investigated its optimal value with different results. When the QEI formulation (Lassabatere et al., 2009) or its expansions (Latorre et al., 2018; Moret-Fernandez et al., 2020) were fitted to synthetic numerical curves generated for the van Genuchten-Mualem (1980) (vGM) soil hydraulic model, β increased from sand to diffusive soil type, exceeding the initially proposed range [0, 1].

The3 extension of the 1D AAP formulation to 3D formulation was performed by introducing the scaling factor γ (Smetten et al., 1994). The combination of the resolution for two-dimensional saturated water flow (known as the Laplace equation) and simplified assumptions such as GA wetting front during the infiltration process leads to a specific theoretical value of $\sqrt{0.3}$ for γ (Smetten et al., 1994). Since this theoretical value was specific to a GA wetting front, the γ value was corrected to 0.75 to fit the 3D formulation to their experimental soil data (Smettem et al., 1994). Then, the 0.75 value for γ became a common value for many studies (Di Prima et al., 2020; Yilmaz et al., 2022a; 2021). However, according to Haverkamp et al. (1994), this parameter should be constrained within the [0.6, 0.8] range.

The proper values of β and γ parameters are the subject of discussion because both are known to depend on soil type and initial water content (Lassabatere et al., 2009, Angulo-Jaramillo et al., 2016)

rather than being considered unique values. No study has focused on the simultaneous estimation of β and γ. In general, the β parameter is prefixed according to measurements performed in a 1D vertical column in the laboratory or directly calculated by the analytical formula of Fuentes et al. (1994). Then γ is adjusted or optimized with the *S* and K_s estimations. Therefore, this paper is novel because it aims to investigate simultaneously the optimal values of β and γ parameters. This approach differs from the others since it doesn't constrain the optimized couplet to 1D flow estimation. For this purpose, numerical cumulative infiltration curves corresponding to six different synthetic soils from the database of Carsel and Parrish (1988) and with contrasting hydraulic behaviors are considered. Hydrus-3D software was used to model cumulative infiltration corresponding to a zero water pressure head at the surface, considering the vGM model for describing the soil hydraulic functions and several initial water contents. The long-time expansion of QEI formulation was used to retrieve the couplet of unknown β and γ for each synthetic soil. Then, the variation of both parameters is discussed in the function of the synthetic soils and initial soil water conditions.

2- Material and Methods

2-1 Soil Hydraulics functions

The van Genuchten model uses the following mathematical function to describe the water retention (Equation 1a) and the hydraulic conductivity (Equation 1b) curves:

$$S_e = \frac{\theta-\theta_r}{\theta_s-\theta_r} = [1+|\alpha h|^n]^{-m} \quad \text{Equation 1a}$$

$$K(\theta) = K_s\left(\frac{\theta-\theta_r}{\theta_s-\theta_r}\right)^l\left[1-\left(1-\left(\frac{\theta-\theta_r}{\theta_s-\theta_r}\right)^{\frac{1}{m}}\right)^m\right]^2 \quad \text{Equation 1b}$$

$$m = 1-\frac{k_m}{n} \quad \text{Equation 1c}$$

Where S_e is the degree of soil water saturation, θ ($L^3\ L^{-3}$) is the volumetric soil water content, h (L) is the water pressure head, K ($L\ T^{-1}$) is the soil hydraulic conductivity, n and m are shape parameters, k_m is a user index (Haverkamp *et al.*, 2016), l is a tortuosity parameter and α (L^{-1}) representing the

inflection point of the water retention curve, θ_s and θ_r ($L^3\ L^{-3}$) are saturated and residual soil volumetric water contents, and K_s ($L\ T^{-1}$) is the field-saturated soil hydraulic conductivity. The Mualem condition (1976) set the k_m parameter to 1 and l to 0.5.

2-2 Synthetic data from Hydrus-3D software

Cumulative Beerkan infiltrations were simulated using HYDRUS-2D/3D software (Šimůnek et al. 2008), which solves Richards' equation governing the flow by applying the finite element method. The numerical domain was configured as a cylinder of 40 cm radius and 40 cm height, representing a volume of 200 dm^3, large enough to contain the wetting front below the ring infiltration device during the whole infiltration process until the attainment of steady-state. Finite elements of 2 mm were used to discretize the numerical domain (Lassabatere et al., 2009). The upper boundary condition was set to saturated water content for the ring section, while the lower boundary limit was set to free drainage condition, and zero flux boundary conditions were applied elsewhere. The ring radius r_d was set to 5 cm. The vGM model and related hydraulic properties of 6 synthetics soils, ranging from sand to silt textures, were used (Table 1). The initial water content was considered homogeneous and set to a degree of saturation S_e of 0, 0.1, 0.2, 0.3, and 0.4. Because of numerical problems for sand and loamy sand, the initial degree of saturation 0 was replaced by 0.05.

2-3 Detection of steady-state

Di Prima et al. (2021) introduced the approach to detect the attainment of steady-state. First, the program considers the last four points of the infiltration curve and then performs a linear regression to calculate the slope. The latter is considered the reference slope. Then the program increments by one the number of points to be considered for the linear regression. At each increment, a threshold E is calculated as follows:

$$E = \frac{slope\_last\_i - slope\_reference}{slope\_reference} < 0.005 \qquad \text{Equation 2}$$

Where $slope\_last\_i$ and $slope\_reference$ values are the measured slope, including the last i^{th} and fourth points, respectively. The points respecting the threshold are considered for the long-time regime. When the threshold value becomes higher than 0.005 for an incremented i number of points, the algorithm stops and considers the steady-state flow process starting at the $i+1$ points of the cumulated infiltration curve.

2-4 Quasi-exact implicit infiltration formulation and its long-time approximation

For a given initial volumetric water content, θ_i, the QEI formulation models the cumulative infiltration at the surface of a single ring of radius r_d (Beerkan type experiment) as below (Haverkamp et al., 1994):

$$\frac{2\Delta K^2}{S^2}t = \frac{1}{1-\beta}\left(\frac{2\Delta K}{S^2}\left(I_{3D} - \frac{\gamma S^2}{r_d(\theta_s-\theta_i)}t - K_i t\right) - \ln\left(\frac{e^{\frac{2\beta\Delta K}{S^2}\left(I_{3D}-\frac{\gamma S^2}{r_d(\theta_s-\theta_i)}t-K_i t\right)}+\beta-1}{\beta}\right)\right) \quad \text{Equation 3}$$

Where t (T) is the time, I_{3D}(L) is the cumulative 3D infiltration, γ is the scaling constant representative of the lateral flow, β is the integration parameter, S (L $T^{-0.5}$) is the initial soil sorptivity, K_i is the initial soil hydraulic conductivity, and ΔK is the difference between the saturated and the initial soil hydraulic conductivity. For long times, the 3D cumulative infiltration, $I_{+\infty}$ (L), can be approximated by the following explicit steady-state expansion (Haverkamp et al., 1994):

$$I_{+\infty}(t) = (AS^2 + \Delta K).t + C\frac{S^2}{\Delta K} \quad \text{Equation 4a}$$

For the specific case of the vGM model, A (L^{-1}) and C constants are defined as:

$$A = \frac{\gamma}{r_d(\theta_S-\theta_i)} \quad \text{Equation 4b}$$

$$C = \frac{1}{2(1-\beta)}\ln\left(\frac{1}{\beta}\right) = \frac{1}{2(1-\beta)}\ln\left(\frac{1}{\beta}\right) \quad \text{Equation 4c}$$

2-5 Reference S calculation, estimation from the steady-state shape, and S error objective function

The reference sorptivity S_{ref} is calculated using the Parlange et al. (1975) flux concentration model as follows:

142 $$S_{ref}^2(\theta_0,\theta_i) = \int_{\theta_i}^{\theta_0}(\theta_0 + \theta - 2\theta_i)D(\theta)\,d\theta$$ Equation 5a

143 Where D stands for the soil diffusivity function. The S_{ref} is calculated for each synthetic soil (Table 1)
144 and initial soil water content using the computation algorithm proposed by Lassabatere et al. (2022).

145 Alternatively, S can be related to the slope and intercept coefficient of equation 4a as follows
146 (Bagarello et al., 2014):

147 $$S = \sqrt{\frac{s_{std}}{A+\frac{C}{i_{std}}}}$$ Equation 5b

148 Where s_{std} and i_{std} stand for the slope and the intercept of the linear regression of the steady-state
149 part of the cumulated infiltration curve. The equation Eq. 5b defines sorptivity as a function of the β
150 and γ parameters. S defined by Eq. 5b must equal S_{ref} as defined by Eq. 5a. We then assess the
151 objective function to calculate the deviation from the reference value as follow:

152 $$S_{error} = S_{ref} - \sqrt{\frac{s_{std}}{A+\frac{C}{i_{std}}}}$$ Equation 5c

153 Accurate values of the β and γ parameters must ensure values of the optimization function close to
154 zero.

155 2-6 K_s estimation from the steady-state and K_s error objective function

156 K_s is estimated from equation 4a using the intercept information (Yilmaz et al., 2010) as follows:

157 $$K_s = \frac{s_{std}}{\left(i_{std}\cdot\frac{A}{C}+1\right)\left(1-\left(\frac{\theta_i-\theta_r}{\theta_s-\theta_r}\right)^{0.5}\left[1-\left(1-\left(\frac{\theta_i-\theta_r}{\theta_s-\theta_r}\right)^{\frac{1}{m}}\right)^{m}\right]^2\right)}$$ Equation 6a

158 The objective function to calculate the deviation from the reference value is defined as follows:

159 $$K_{s_{error}} = K_{s_{ref}} - \frac{s_{std}}{\left(i_{std}\cdot\frac{A}{C}+1\right)\left(1-\left(\frac{\theta_i-\theta_r}{\theta_s-\theta_r}\right)^{0.5}\left[1-\left(1-\left(\frac{\theta_i-\theta_r}{\theta_s-\theta_r}\right)^{\frac{1}{m}}\right)^{m}\right]^2\right)}$$ Equation 6b

Again, accurate values of the β and γ parameters must ensure values of the optimization function close to zero. We have then defined two objective functions that allow retrieving the best values of the β and γ parameters.

2-7 Contours of the minimum of K_s and S error objective function

K_s and S are estimated for (β, γ) couplets ranging each term from 0.1 to 3 with an increment step of 0.005. Thus, the objective function is calculated for each couplet to find the minimum. Crossing the objective functions thus takes up the values of (β, γ) couplet that best fits with the values of references K_s and S. Since the objective functions (5a and 6b) are derived from the shape coefficient of the steady-state, the calculation of the values of (β, γ) are done from the shape coefficient as described after.

2-8 Estimation of (β, γ) couplet from shape coefficient

The γ value is calculated by considering the relation 4a with the reference values K_s and S, and the slope of the linear regression of the steady-state points as follows:

$$\gamma = \frac{r_d(\theta_s - \theta_i)\left(s_{std} - K_{s_{ref}}\right)}{S_{ref}^2} \qquad \text{Equation 7a}$$

In order to calculate the β value, the intercept of the regression line of the steady-state is used to define a new objective function f, as follows:

$$f(\beta) = i_{std} - \frac{1}{2(1-\beta)\left(1-\left(\frac{\theta_i - \theta_r}{\theta_s - \theta_r}\right)^{0.5}\left[1-\left(1-\left(\frac{\theta_i - \theta_r}{\theta_s - \theta_r}\right)^{\frac{1}{m}}\right)^{m}\right]^2\right)} \ln\left(\frac{1}{\beta}\right)\frac{S_{ref}^2}{K_{s_{ref}}} \qquad \text{Equation 7b}$$

Then Scilab "fsolve" function (Campbell et al., 2010), which finds the zero for a mathematical function, is used to retrieve the equivalent β. The values computed of the (β, γ) couplet computed with Eqs 7a and 7b correspond to the optimum values of the objective functions defined by Eqs 5c and 5c.

2-9 Relative error estimation of S and K_s using by-default (β, γ) couplet

To highlight the bias in the estimation of S and K_s with respect to their reference value, when the by-default ($\beta = 0.6, \gamma = 0.75$) couplet is used, the relative error [%] is calculated as follows:

$$S_{relative\ Error} = \frac{S_{estimated} - S_{ref}}{S_{ref}} \times 100 \quad \text{Equation 8a}$$

$$K_{s_{relative\ Error}} = \frac{K_{s_{estimated}} - K_{s_{ref}}}{K_{s_{ref}}} \times 100 \quad \text{Equation 8b}$$

3 – Results

3-1 Beerkan cumulative infiltrations and steady-state asymptotes

Simulations for the six synthetic soils and the different scenarios of initial water content are shown in Figure 1. The steady-state attainment time, t_{std}, asymptote slope, s_{std}, and intercept, i_{std}, are summarized in Table 2.

3-2 Contour of objectives functions

The contours of the objective error functions for S (Eq. 5c) and K_s (Eq. 6b) and the intersection of both contour error lines of 0.005 for initial saturation degree $S_e = 0.1$ are illustrated in Figure 2. The crossing pattern (Right column, Figure 2) shows the (β, γ) couplet that fits well with both expected S and K_s values. Their exact values were calculated from steady state shape coefficients and summarized in Table 2 (Cf. the last two columns).

3-3 Relative error of S and K_s estimates using by-default values of (β, γ) couplet

Using the by-default value of 0.6 and 0.75 for (β, γ) couplet resulted in relative errors for S estimate below 2 %, in absolute value, for sand, loamy sand, and sandy loam (Table 2). For the others, the error was constrained below 10 % in absolute value. For K_s estimates, the relative errors were higher than for S estimates. The minimum error range was observed for sandy loam in the range of [4.7-11.1] %, and the maximum error was for silt in the range of [32.1-70.4] % in function to the initial degree of saturation.

204 3-3 Identification of (β, γ) couplet from steady-state measurements

205 For initial conditions of $S_e = 0.1$, parameter β depends on the soil texture and decreases from 1.01 to
206 0.77, respectively, for sand and sandy loam and then increases to 2.32 for silt (Table 2). This parameter
207 also increases from dry to wetter initial conditions for loamy sand, whereas it decreases for the other
208 synthetic soils.

209 The value of the γ parameter for an initial degree of saturation of 0.1 decreases from 0.98 to 0.76 for
210 sand and loam, respectively, and then it slightly increases to 0.79 for silt. For sand and loamy sand, γ
211 optimized values slightly increase from dry to wetter initial conditions and decrease for the remaining
212 soils.

213 4- Discussion

214 4-1 Effect of the by-default couplet value on the estimates of K_s and S

215 The objective error function for K_s (Figure 2) obtained from the steady-state approach (Equation 4a)
216 shows an increasing elongated valley, which indicates that infinite values of the couplet (β, γ) can be
217 chosen for the actual estimate of K_s. A similar behavior, with a decreasing elongated valley, was
218 observed in the estimates of S. Simultaneous estimate of both parameters conducts to a restricted
219 choice of the couplet (β, γ) represented by the intersection of both valleys with minimum error.
220 Identifying the intersection of the two zones correctly identifies the optimum values of the couplet
221 (β, γ) and are directly calculated from equations 7a and 7b. Therefore, it is interesting to test the by-
222 default (β, γ) couplet value to see the potential errors in the estimation of S and K_s (Table 2). In such
223 case and considering the field variability of intrinsic soil parameters such as porosity, the relative errors
224 observed for S are negligible (< 10%). For the estimation of K_s, the observed relative error is higher
225 than S, but indicates that the estimates remain in the same order of magnitude as the reference value
226 (< 60%). The case of synthetic sandy loam, with the by-default couplet (β, γ), led to the smallest errors.
227 That seems logical since the original default values were calculated for cumulative infiltration curves
228 experimentally measured for sandy loam soils in the laboratory (Smettem et al., 1994) and on the field

(Haverkamp et al., 1994). Globally, for a more rigorous estimation of the K_s parameter, the couplet (β, γ) must be corrected according to the soil type and initial soil moisture content.

4-2 Comparison to values of couplet (β, γ) reported in the literature

In the literature, almost all studies that employ the QEI formulation (Haverkamp et al., 1994) and its corresponding expansions systematically used the by-default (β, γ) values. Note that BEST methods (Yilmaz et al., 2019; Di Prima et al., 2021) and the simplified Beerkan approach (Yilmaz, 2021; Di Prima et al., 2020; Bagarello et al., 2017) used a different model for the modeling of hydraulic functions, i.e., the van Genuchten (1980) model for the water retention curve and the Brooks and Corey (1967) model for the unsaturated hydraulic conductivity (Lassabatere et al., 2021). Therefore, the conclusion of this study may not apply to these methods since we investigated values of (β, γ) for the specific case of the vGM model. However, we may expect similar trends. Further investigations will deal with the dependency of our findings on the mathematical formulations considered for the description of the water retention and hydraulic conductivity functions.

Few studies have evaluated the effect of β and γ parameters on the estimates of K_s and S (Table 3), focusing mainly on initial very dry conditions. Our study differs from these in that we analyzed the cumulative infiltration at long times, we estimate simultaneously both parameters β and γ rather than fixing β from 1D and adjusting γ value. In complement, we also investigate the effect of initial soil moisture from dry to wet conditions on both parameters. For instance, Latorre et al. (2018) observed that β could be accurately estimated with QEI formulation from a single infiltration curve only when very long times were considered. Once β is estimated then they extrapolated the 1D results to 3D flow. Similar approach was done by Lassabatere et al. 2009. Working with QEI expansions, Moret-Fernandez et al. (2020) and Rahmati et al. (2020) prefixed β according to textural parameters and 1D analytical formulation of Fuentes (1992). They observed that β had a meager impact on the K_s and S estimates. However, using the long-time formulation, we observed that the β parameter has a direct influence on the coefficient *C* (Equation 4c), which directly influences the estimation of K_s and S. This

results in significant differences between the β values in the literature obtained from 1D flow conditions and those found in this work for 3D flow conditions.

For sand synthetic soil, the β value observed for initially relatively dry soils was close to 1.02. This value differs from the study of Lassabatere et al. (2009) , Rahmati et al. (2020), Moret-Fernandez and Latorre (2017), who observed β value between 0.33 and 0.6. Note that although Moret-Fernandez et al. (2020) considered β value of 0.6 for sandy soils from inversion of 1D infiltration experiments, for 3D infiltration, the β value observed in their optimization procedure was close to 1. This clearly shows differences between the 1D and 3D β estimates and calls into question the extrapolation of β from 1D flow to estimate soil parameters from 3D flow.

For the γ parameter, our observed values are close to those proposed by Lassabatere et al. (2009). Moreover, Moret-Fernandez et al. (2020) reused the γ value for loam soil and observed similar optimized values of β in comparison to our steady-state approach. Haverkamp et al. (1994) bounded γ parameter between 0.6 and 0.8 for "normal working conditions". This statement is vague since "normal working condition" is not explicit. It seems that for very permeable soil, such as sand and loamy sand, this range can be expanded and be closer to 1.

4-3 Effect of the initial soil water content

4-3-1 On the estimate of S and K_s using the by-default couplet (β, γ)

Regarding the effect of the initial water content with the by-default couplet (β, γ), a similar error was obtained in the estimation of S, regardless of the initial soil water content (Table 2). Therefore, no effect of the initial water content was observed for this parameter. Contrary to the estimation of K_s, the increase of the initial water content resulted in an increase or a decrease in the error according to the soil type (Table 2). For instance, for sand and loamy soils, the error of K_s remains almost stable with the increase of the initial soil degree saturation. This trend contrast with the remaining soils,

where a decrease of the K_s error with the increase of the initial soil degree saturation was observed. Therefore, the studied synthetic soils could be classified into two groups: sand and loamy sand soils on the one hand, and sandy loam, loam, silty loam, and silt soil on the other hand, with regard to the impact of the by-default value on the estimations of S and K_s. The evolution of the optimum values of the couplet (β, γ) is then discussed afterwards.

4-3-1 On the optimized value of (β, γ)

For the first group, β and γ values increase with increasing initial water content. It should be noted that the increase of γ is contained in a small range (Table 2) compared to β and can be considered almost constant. For the second group, we have an opposite effect where β and γ values decrease with the increase of the initial water content. It should be noted that for the sandy loam, the γ value remains almost constant as well.

During field experiments, utterly dry condition such as initial degree of saturation below 0.1 is rarely observed and infiltration tests are generally performed with initial soil condition higher but remaining relatively dry ($Se_i < 0.3$). Therefore, some values of β and γ can be considered for the estimation of S and K_s. For the first group (sand and loamy sand textural soils), γ can be set to 0.9. Indeed, it is logical for very permeable soils to have a revised γ value higher than 0.75 because these soils have a behavior quite close to a 1D flow. While for the second group, a default value of 0.75 can be kept. For the β parameter, the first group can have a value close to 0.9 which represents a mean value for this group. However, for the second group, it is not possible to fix a mean value for β value beforehand, as it varies from 0.72 to 2.32. Therefore, we propose to split this group in two: sandy loam textural soils and the others (Loam, silty loam and silt) with respectively β values fixed to 0.75 and 1.5.

5- Conclusions

In the debate on the constancy of the couplet (β, γ), this study showed that these parameters are not constant and are influenced by the type of soil and the initial soil moisture. Our results indicate that synthetic soils can be classified into three groups: very draining soils with a reach of the permanent

303 regime in less than 30 minutes (sand and loamy sand textural type), the second group where regime
304 permanent is reached in less than 120 minutes (sandy loam textural type) and the others. For the first
305 group and for relatively initially dry soil conditions (i.e., $Se_i < 0.3$), we suggest readjusting the by-
306 default couplet from the case of ($\beta = 0.6, \gamma = 0.75$) to ($\beta = 0.9, \gamma = 0.9$). Note that the value of $\beta =$
307 1 cannot be considered since it may lead to undefined numerical values with the use of the QEI model
308 (see Eq. 3) or the definition of the asymptote intercept (see Eq. 4). For the second group (sandy loam
309 textural soils), we propose to readjust the couplet to ($\beta = 0.75$, $\gamma = 0.75$). For the last group who
310 requests longer times for the attainment of the steady state flow (over 120 minutes), the values ($\beta =$
311 $1.5, \gamma = 0.75$) can be chosen as a good option for a more precise estimation of S and K_s. The results
312 of this investigation are specific to the case of van Genuchten-Mualem soil hydraulic models and need
313 to be tested on other models before generalization. The present work also highlights that there are
314 two good options for the definition of the γ constant with 0.9 and 0.75. This means that a pre-fixed
315 value for γ can be used when the transient expansion 3, 4, and 5 terms of the QEI and simultaneous
316 estimate of triplet (K_s, S, β) are considered. Although this work has focused on soil textural
317 characteristics, new efforts should be made to study the possible influence of soil structure, for
318 instance, compacted soils or high porosity soils such as technosols (Yilmaz et al., 2022b) on β and γ
319 values.

320

6- References

Angulo-Jaramillo, R., Bagarello, V., Iovino, M., & Lassabatere, L. (2016). Infiltration measurements for soil hydraulic characterization. Berlin, Germany: Springer.

Bagarello, V., Di Prima, S., Iovino, M., 2014. Comparing Alternative Algorithms to Analyze the Beerkan Infiltration Experiment. Soil Science Society of America Journal 78, 724. https://doi.org/10.2136/sssaj2013.06.0231

Bagarello, V., Di Prima, S., & Iovino, M. (2017). Estimating saturated soil hydraulic conductivity by the near steady-state phase of a Beerkan infiltration test. Geoderma, 303, 70-77. https://doi.org/10.1016/j.geoderma.2017.04.030

Campbell, S. L., Chancelier, J. P., & Nikoukhah, R. (2010). Modeling and Simulation in SCILAB. In Modeling and Simulation in Scilab/Scicos with ScicosLab 4.4 (pp. 73-106). Springer, New York, NY.

Di Prima, S., Stewart, R. D., Castellini, M., Bagarello, V., Abou Najm, M. R., Pirastru, M., Giadrossich, F., Iovino, M., Angulo-Jaramillo, R., & Lassabatere, L. (2020). Estimating the macroscopic capillary length from Beerkan infiltration experiments and its impact on saturated soil hydraulic conductivity predictions. Journal of Hydrology, 589, 125159. https://doi.org/10.1016/j.jhydrol.2020.125159

Di Prima, S., Stewart, R.D., Abou Najm, M.R., Ribeiro Roder, Giadrossich, F., Campus, S., Angulo-Jaramillo, R., Yilmaz, D., Rogerro, P.P., Pirastru, M., Lassabatere, L., 2021. BEST-WR: an adapted algorithm for the hydraulic characterization of hydrophilic and water-repellent soils. Journal of Hydrology 603, 126936. https://doi.org/10.1016/j.jhydrol.2021.126936

Fuentes, C., Haverkamp, R., & Parlange, J. Y. (1992). Parameter constraints on closed-form soilwater relationships. Journal of hydrology, 134(1-4), 117-142. https://doi.org/10.1016/0022-1694(92)90032-Q

Haverkamp, R., Parlange, J. Y., Starr, J. L., Schmitz, G., & Fuentes, C. (1990). Infiltration under ponded conditions: 3. A predictive equation based on physical parameters. Soil science, 149(5), 292-300. https://doi.org/10.1097/00010694-199005000-00006

Haverkamp, R., Ross, P. J., Smettem, K. R. J., & Parlange, J. Y. (1994). Three-dimensional analysis of infiltration from the disc infiltrometer: 2. Physically based infiltration equation. Water Resources Research, 30(11), 2931-2935. https://doi.org/10.1029/94WR01788

Haverkamp, R., Bouradui, F., Zammit, C., & Angulo-Jaramillo, R. (1999). Movement of moisture in the unsaturated zone. Groundwater engineering handbook. CRC, Boca Raton, Fla.

Haverkamp, R., Debionne, S., Angulo-Jaramillo, R., & de Condappa, D. (2016). Soil properties and moisture movement in the unsaturated zone. In The handbook of groundwater engineering (pp. 167-208). CRC Press.

Lassabatere, L., Angulo-Jaramillo, R., Soria-Ugalde, J. M., Šimůnek, J., & Haverkamp, R. (2009). Numerical evaluation of a set of analytical infiltration equations. Water Resources Research, 45(12). https://doi.org/10.1029/2009WR007941

Lassabatere, L., Peyneau, P. E., Yilmaz, D., Pollacco, J., Fernández-Gálvez, J., Latorre, B., Moret-Fernández, D., Di Prima, S., Rahmati, M., Stewart, R.D, Abou Najm, M., Hammecker, C. & Angulo-Jaramillo, R. (2021). Scaling procedure for straightforward computation of sorptivity. Hydrology and Earth System Sciences, 25(9), 5083-5104. https://doi.org/10.5194/hess-25-5083-2021

Lassabatere, L., Peyneau, P. E., Yilmaz, D., Pollacco, J., Fernández-Gálvez, J., Latorre, B., Moret-Fernández, D., Di Prima, S., Rahmati, M., Stewart, R.D, Abou Najm, M., Hammecker, C. & Angulo-Jaramillo, R. (2022). Mixed formulation for an easy and robust numerical computation of sorptivity. Hydrology and Earth System Sciences, Preprint hess-2021-633. https://doi.org/10.5194/hess-2021-633

Latorre, B., Moret-Fernández, D., Lassabatere, L., Rahmati, M., López, M. V., Angulo-Jaramillo, R., Sorando, R., Comin, F., & Jiménez, J. J. (2018). Influence of the β parameter of the Haverkamp model on the transient soil water infiltration curve. Journal of Hydrology, 564, 222-229. https://doi.org/10.1016/j.jhydrol.2018.07.006

Moret-Fernández, D., & Latorre, B. (2017). Estimate of the soil water retention curve from the sorptivity and β parameter calculated from an upward infiltration experiment. Journal of Hydrology, 544, 352-362. https://doi.org/10.1016/j.jhydrol.2016.11.035

Moret-Fernández, D., Latorre, B., López, M. V., Pueyo, Y., Lassabatere, L., Angulo-Jaramilo, R., Rahmati, M., Torma, J., & Nicolau, J. M. (2020). Three-and four-term approximate expansions of the Haverkamp formulation to estimate soil hydraulic properties from disc infiltrometer measurements. Hydrological Processes, 34(26), 5543-5556. https://doi.org/10.1002/hyp.13966

Mualem, Y. (1976). A new model for predicting the hydraulic conductivity of unsaturated porous media. Water resources research, 12(3), 513-522. https://doi.org/10.1029/WR012i003p00513

Parlange, J. Y. (1975). On solving the flow equation in unsaturated soils by optimization: Horizontal infiltration. Soil Science Society of America Journal, 39(3), 415-418. https://doi.org/10.2136/sssaj1975.03615995003900030019x

Parlange, J. Y., Lisle, I., Braddock, R. D., & Smith, R. E. (1982). The three-parameter infiltration equation. Soil Science, 133(6), 337-341. https://doi.org/10.1097/00010694-198206000-00001

Rahmati, M., Vanderborght, J., Simunek, J., Vrugt, J. A., Moret-Fernández, D., Latorre, B., Lassabatere, L., & Vereecken, H. (2020). Soil hydraulic properties estimation from one-dimensional infiltration experiments using characteristic time concept. Vadose Zone Journal, 19(1). https://doi.org/10.1002/vzj2.20068

Ross, P. J., Haverkamp, R., & Parlange, J. Y. (1996). Calculating parameters for infiltration equations from soil hydraulic functions. Transport in porous media, 24(3), 315-339. https://doi.org/10.1007/BF00154096

Šimůnek, J., van Genuchten, M. T., & Šejna, M. (2008). Development and applications of the HYDRUS and STANMOD software packages and related codes. Vadose Zone Journal, 7(2), 587-600. https://doi.org/10.2136/vzj2007.0077

Smettem, K. R. J., Parlange, J. Y., Ross, P. J., & Haverkamp, R. (1994). Three-dimensional analysis of infiltration from the disc infiltrometer: 1. A capillary-based theory. Water Resources Research, 30(11), 2925-2929. https://doi.org/10.1029/94WR01787

Van Genuchten, M. T. (1980). A closed-form equation for predicting the hydraulic conductivity of unsaturated soils. Soil science society of America journal, 44(5), 892-898. https://doi.org/10.2136/sssaj1980.03615995004400050002x

Yilmaz, D., Lassabatere, L., Angulo-Jaramillo, R., Deneele, D., Legret, M., 2010. Hydrodynamic Characterization of Basic Oxygen Furnace Slag through an Adapted BEST Method. Vadose Zone Journal 9, 107. https://doi.org/10.2136/vzj2009.0039

Yilmaz, D., Bouarafa, S., Peyneau, P.E., Angulo-Jaramillo R., Lassabatere, L., 2019. Assessment of hydraulic properties of technosols using Beerkan and multiple tension disc infiltration methods. European Journal of Soil Science, 70, 1049-1062. https://doi.org/10.1111/ejss.12791

Yilmaz, D. (2021). Alternative α* Parameter Estimation for Simplified Beerkan Infiltration Method to Assess Soil Saturated Hydraulic Conductivity. Eurasian Soil Science, 54, 1049-1058. https://doi.org/10.1134/S1064229321070140

Yilmaz, D., Di Prima, S., Stewart, R.D., Abou Najm, M.R., Fernandez-Moret, D., Latorre, B., & Lassabatere, L. (2022a). Three-term formulation to describe infiltration in water-repellent soils. Geoderma, 427, 116127. https://doi.org/10.1016/j.geoderma.2022.116127

Yilmaz, D. (2022b). Testing Simplified Beerkan Infiltration (SBI) Methods on Technosol to Estimate the Saturated Hydraulic Conductivity. Geotechnical and Geological Engineering, 40, 2897-2906. https://doi.org/10.1007/s10706-022-02074-0

417 7- Tables

418 Table 1. vGM related hydraulic parameters for the six studied synthetic soils (Di Prima et al., 2021)

Type of soil	θ_r	θ_s	n	α (cm^{-1})	K_s (cm.min^{-1})	t_f (min)
Sand	0.045	0.430	2.68	0.145	0.495	30
Loamy Sand	0.057	0.410	2.28	0.124	0.2432	60
Sandy Loam	0.065	0.410	1.89	0.075	0.07368	120
Loam	0.078	0.430	1.56	0.036	0.01733	240
Silty Loam	0.067	0.450	1.41	0.02	0.00750	480
Silt	0.034	0.460	1.37	0.016	0.00417	720

419

420

421

Table 2. Summary of asymptote slope and intercept, relative error on S and K_s using by-default (β, γ) estimated optimum values of (β, γ)

	S_{e_i} [-]	t_{std} [min]	s_{std} [mm.min^{-1}]	i_{std} [mm]	S Eq. 5a [mm.min$^{-0.5}$]	S_{Error} Eq. 8a [%]	$K_{s_{Error}}$ Eq. 8b [%]	β Eq. 7b	γ Eq. 7a
Sand	0.05	11.3	1.198	1.319	1.148	0.8	31.0	1.020	0.975
	0.1	11.7	1.197	1.251	1.116	0.9	30.9	1.012	0.976
	0.2	9.4	1.197	1.090	1.049	0.7	32.2	1.042	0.982
	0.3	7.5	1.196	0.934	0.977	0.5	33.9	1.076	0.990
Loamy Sand	0.05	23.5	0.561	1.378	0.773	1.5	17.3	0.792	0.890
	0.1	23.2	0.560	1.302	0.752	1.5	17.4	0.793	0.892
	0.2	19.8	0.560	1.141	0.706	1.4	18.1	0.806	0.896
	0.3	17.9	0.559	0.989	0.658	1.6	18.7	0.809	0.902
	0.4	15.8	0.558	0.835	0.605	1.8	20.2	0.821	0.913
Sandy Loam	0	68.3	0.184	1.835	0.491	-1.3	11.1	0.794	0.789
	0.1	64.5	0.183	1.667	0.465	-1.1	10.0	0.770	0.787
	0.2	64.9	0.182	1.515	0.437	-0.5	8.1	0.725	0.786
	0.3	64.0	0.181	1.369	0.407	0.4	5.6	0.665	0.785
	0.4	55.0	0.180	1.185	0.374	1.0	4.7	0.635	0.789
Loam	0	159.0	0.053	1.944	0.285	-7.2	32.1	1.429	0.766
	0.1	161.0	0.052	1.814	0.269	-6.9	27.8	1.322	0.756
	0.2	167.0	0.051	1.688	0.253	-6.3	22.8	1.196	0.746
	0.3	159.0	0.051	1.534	0.236	-5.8	18.6	1.093	0.738
	0.4	155.0	0.050	1.362	0.217	-5.2	14.6	0.996	0.731
Silty Loam	0	338.0	0.028	2.337	0.222	-8.5	50.8	1.923	0.775
	0.1	327.0	0.027	2.182	0.211	-8.4	45.3	1.785	0.761
	0.2	328.0	0.027	2.019	0.198	-8.0	39.8	1.642	0.751
	0.3	346.0	0.026	1.867	0.185	-7.5	32.9	1.462	0.738
	0.4	266.0	0.026	1.591	0.170	-7.5	32.1	1.448	0.737
Silt	0	560.0	0.017	2.511	0.184	-9.4	70.4	2.465	0.800
	0.1	556.0	0.017	2.332	0.175	-9.3	64.6	2.317	0.786
	0.2	525.0	0.016	2.127	0.164	-9.2	60.1	2.193	0.777
	0.3	523.0	0.016	1.944	0.153	-8.8	53.4	2.004	0.765
	0.4	266.0	0.026	1.591	0.170	-7.5	32.1	1.813	0.737

422

423

Table 3. Literature summary of optimized β or/and γ parameters on numerical curves produced with vGM model from Hydrus software and QEI formulation and its expansions.

	Synthetic Soil	β	γ
Lassabatere et al. (2009)- From QEI 3D infiltration	Sand	0.33	1.030
	Loam	1.25	0.756
	Silt	1.56	0.748
Moret-Fernandez and Latorre (2017)- From Upward 1D infiltration	Sand	0.63	
	Loam	1.25	
	Silt	1.56	
Latorre et al. (2018) - From AAP 1D infiltration	Loamy sand	0.78	
	Loam	1.27	
	Silt	1.50	
Moret-Fernandez et al. (2020)- From QEI 3D infiltration	Sand	0.63	1.030
	Loam	1.25	0.756
	Silt	1.56	0.748
Rahmati et al. (2020) - From 5T expansion of AAP 1D infiltration	Sand	0.60	
	Loamy Sand	0.80	
	Sandy Loam	0.99	
	Loam	1.27	
	Silty Loam	1.44	
	Silt	1.50	

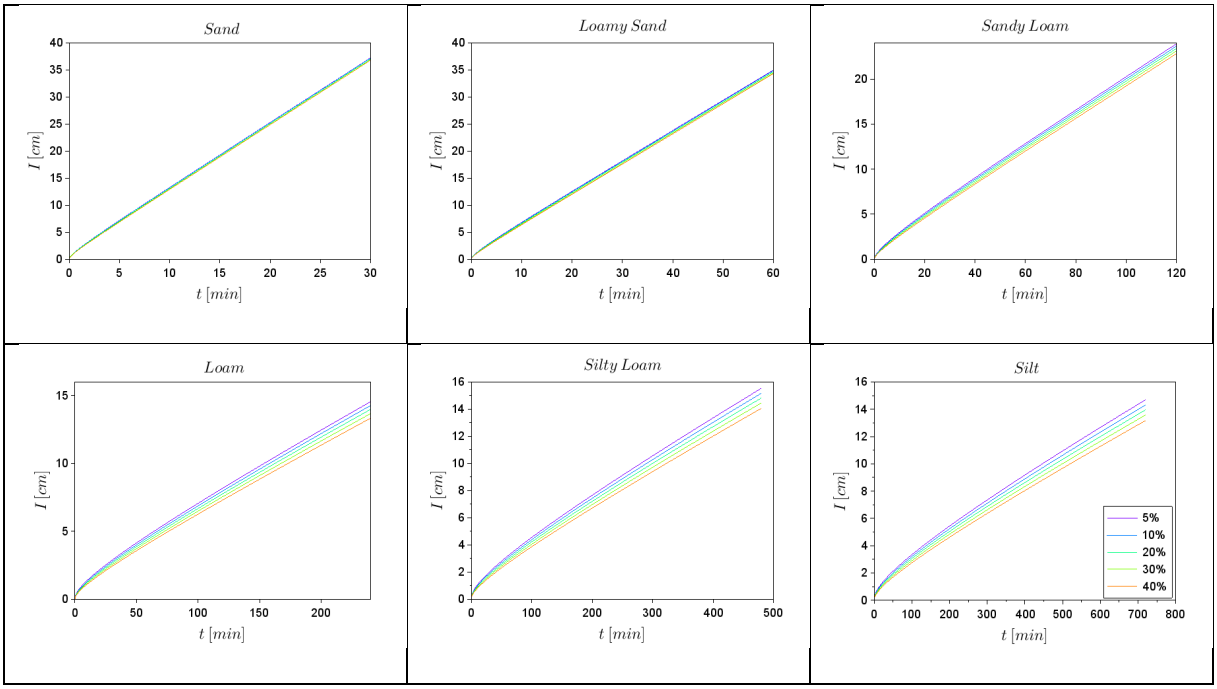

Figure 1. Numerical Hydrus cumulative infiltration calculated for the six synthetic soils and scenarios of initial soil volumetric water content of 5, 10, 20, 30 and 40 % of the effective volumetric water content (θs- θr).

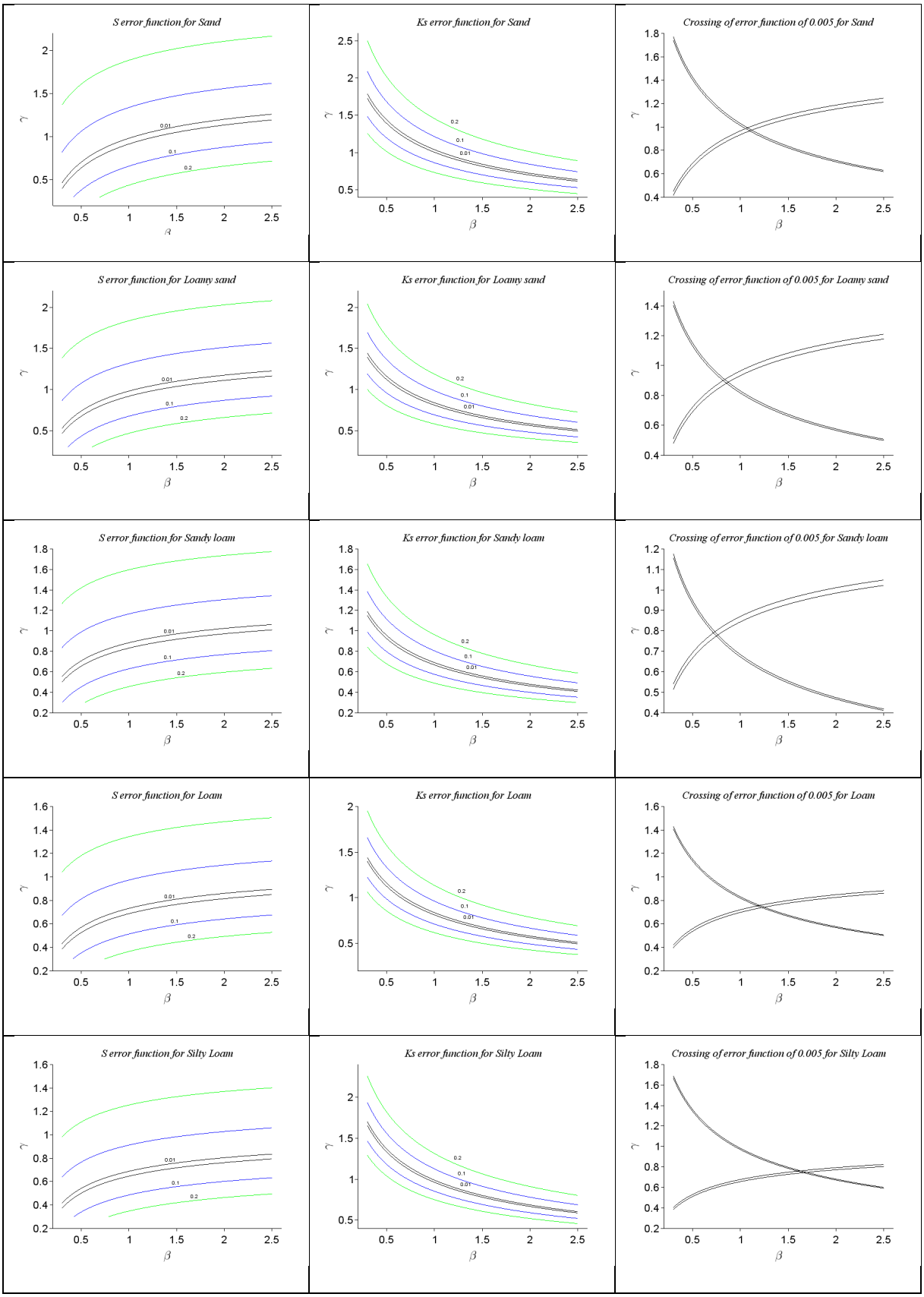
S error function for Sand
Ks error function for Sand
Crossing of error function of 0.005 for Sand
S error function for Loamy sand
Ks error function for Loamy sand
Crossing of error function of 0.005 for Loamy sand
S error function for Sandy loam
Ks error function for Sandy loam
Crossing of error function of 0.005 for Sandy loam
S error function for Loam
Ks error function for Loam
Crossing of error function of 0.005 for Loam
S error function for Silty Loam
Ks error function for Silty Loam
Crossing of error function of 0.005 for Silty Loam
γ
β
0.01
0.1
0.2

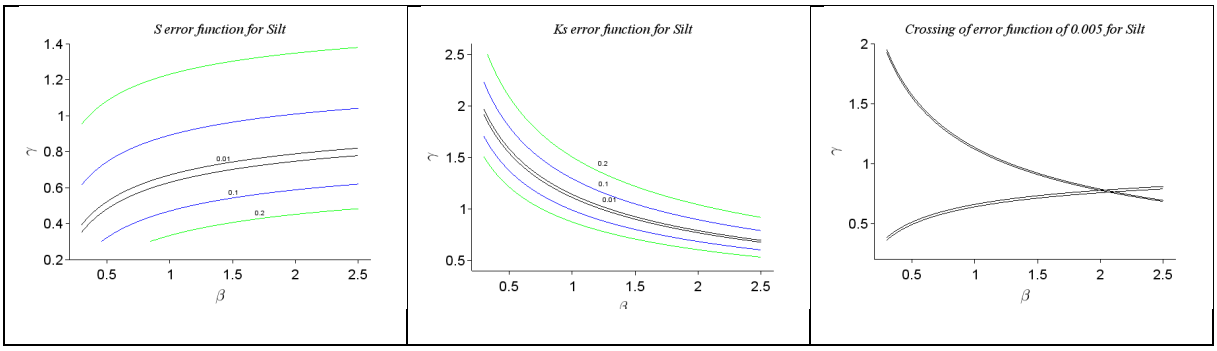

Figure 2. S and Ks error functions contours for 0.1 initial degree of saturation, (green, blue and black lines represent error value of 0.2, 0.1 and 0.01, respectively), and error functions intersection for S and K_s and for 0.005 error value.